Polymer Testing 124 (2023) 108086

Contents lists available at ScienceDirect

Polymer Testing

journal homepage: www.elsevier.com/locate/polytest

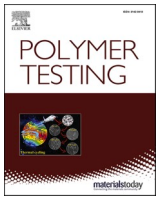

Molecular degradation mechanism of segmented polyurethane and life prediction through accelerated aging test

Sangjun Hong [a,b], Na-young Park [c], Sanghyeon Ju [a], Ajeong Lee [a], Youngeun Shin [a], Jung Soo Kim [a], Moon-Kwang Um [a], Jin Woo Yi [a], Han Gi Chae [b,**], Teahoon Park [a,*]

[a] Carbon Composite Department, Composites Research Division, Korea Institute of Materials Science (KIMS), 797, Changwon-daero, Seongsan-gu, Changwon-si, Gyeongsangnam-do, 51508, Republic of Korea
[b] School of Materials Science and Technology, Ulsan National Institute of Science and Technology (UNIST), 50 UNIST-gil, Ulsan, 44919, Republic of Korea
[c] LIG NEX1 Co., Ltd, 354-25, Sanho-daero, Gumi-si, Gyeongsangbuk-do, Republic of Korea

ARTICLE INFO

Keywords:
Life estimation
Segmented polyurethane
Glycolysis
Accelerated aging
Depolymerization

ABSTRACT

Polyurethane (PU) has numerous applications in daily life, such as coating, cushions, and insulation materials. It is also used as an encapsulation material for sensors. In the case of PU used as an encapsulant, PU elastomer containing an ether-based polyol is generally used and has a long lifespan in a general environment. However, it is challenging to predict its lifespan when used as an encapsulation material for sonar sensors because PU is exposed to the filling liquid. It is required to accurately predict the encapsulation material's lifespan to ensure the sensor's safety. For the exact estimation of PU lifespan, an accelerated aging experiment was conducted on PU elastomer in a filling solution at various temperatures. Fourier transform infrared spectroscopy was used to track the chemical changes in the PU elastomer, and it was observed that both urethane and urea bonds were degraded. Modulated differential scanning calorimetry and thermogravimetric analysis were also used to study changes in the structure of PU elastomer by heat aging. The tensile strength, elongation, and hardness of the heat-aged elastomer at various temperatures were obtained, and the Arrhenius plots were constructed. Finally, the lifespan was considered when the tensile strength was 70% of the initial state by using the ASTM D2000 standard. Thus, the lifespan of PU at 25 °C was calculated to be 12.2 years.

1. Introduction

Polyurethane (PU) was developed by Otto Bayer in 1937 to compete with nylon. It is produced using two raw materials: polyol and diisocyanate. This polymer is characterized by its versatility. Its physical properties can be freely controlled via the type of raw material. It can have high tensile strength and rigidity or, conversely, high flexibility and ductility. In addition, PU has a wide range of applications and reliability owing to its excellent physical properties. A low-density PU elastomer is used for footwear, and a rigid PU elastomer is used for electronic instrument bezels [1–5].

PU elastomer has also been used as an encapsulation material for sonar sensors [6–8]. For encapsulation, the speed of the sound waves before and after transmission should not be changed. In other words, the speed of the sound waves in the encapsulation materials should be the same as that in seawater. Second, the mechanical properties should be reliable. The encapsulation materials protect the inside of the sensor from other impacts, such as sloshing and sea waves. Additionally, materials should have less degradation or loss of properties by seawater or container solution by their high physical and chemical resistance. PU is a suitable material that satisfies these requirements [9]. In addition, the versatile properties of PU also serve as a significant advantage in this application. In the military field, a sonar sensor with PU elastomer encapsulation is generally located on the head of missiles, and the missiles are placed in the filling liquid and stored in a container before launching. The filling solution can be varied by mixing different solutions and additives, depending on the specific purpose. Among the different types of mixtures, they should have anti-freezing properties to

Abbreviations: PU, polyurathene; THF, tetrahydrofuran; PTMEG, Poly(tetramethylene ether) glycol; TDI, toluene diisocyanate; MBOCA, 4,4′-methylene-bis-2-chloroaniline; FT-IR, Fourier transform infrared; MDSC, Modulated differential scanning calorimetry; TGA, Thermogravimetric analysis.

* Corresponding author.
** Corresponding author.
E-mail addresses: hgchae@unist.ac.kr (H.G. Chae), thpark@kims.re.kr (T. Park).

https://doi.org/10.1016/j.polymertesting.2023.108086
Received 25 March 2023; Received in revised form 3 May 2023; Accepted 25 May 2023
Available online 2 June 2023

minimize damage from icing. Therefore, similar to automobiles, glycol and water are used as filling solutions [10,11].

However, PU is also sensitive to hydrolysis and glycolysis [12–14]. For example, the sole of a shoe produced of urethane crumbles owing to decomposition by hydrolysis. Therefore, for the encapsulation application of the sonar sensor, the hydrolysis and glycolysis of the PU layers under storage solution conditions should be accurately studied. It is particularly important to calculate the rate and mechanism of heat aging via glycolysis. The lifespan of PU elastomer must be precisely calculated to determine when to replace the molding material. If PU elastomer is used after a proper lifespan, cracks may occur and damage the internal sensor or cause a change in the sound wave transmission speed, resulting in negative results.

Regarding the chemical structure of PU, there are three main types of PU, which are polymerized using ester, ether, and carbonate-based polyols. When PU elastomer is manufactured using an ester-based polyol, the mechanical properties are sufficiently favorable, but the ester group is weak for hydrolysis, and most of the physical properties are lost in a short period [14–18]. Although PU comprising carbonate units are more resistant to decomposition under water conditions, their use is limited by the high price and complex synthesis methods. Therefore, it is preferable to use ether polyols to make PU elastomers. This is because the ether unit has a higher chemical resistance than the ester owing to dipole–dipole interactions.

When a tetrahydrofuran (THF)-based polyol is used, elastomer has excellent mechanical properties, elasticity, and hydrolysis resistance [19,20]. In this work, an ether-based polyol obtained from THF was used to synthesize PU elastomer, and an accelerated aging experiment was designed to characterize the physical properties and analyze the chemical decomposition mechanism [21–25]. The result of the mechanical test showed a decrease in tensile strength by increasing the heat-aging time. However, unlike in the case of general elastomer, the value of the elongation at the break initially showed an upward trend before a decrease. This study emphasizes the reason for this trend which is not discussed before. Through this accelerated heat-aging test, it is possible to predict the lifespan of PU elastomer at room temperature using Arrhenius plots [26].

2. Experiment

2.1. Preparation of PU elastomer

PU elastomer was synthesized using a prepolymer and curing agent. Poly(tetramethylene ether) glycol glycol (PTMEG, M_n ~2000) and toluene diisocyanate (TDI) were purchased from Sigma-Aldrich and used to prepare the prepolymers. The curing agent mainly consisted of 4,4′-methylene-bis-2-chloroaniline (MBOCA). The prepolymer and MBOCA were reacted at 110 °C for 1.5 h in a mold. Afterward, the synthesized elastomer was post-cured at 110 °C for 1.5 h to obtain a urethane elastomer with Shore A hardness of 85 or more (weight distribution of pristine PU elastomers is shown in Fig. S1, and the hardness of the PU elastomers is shown in Fig. S2).

2.2. Preparation of heat-aging and filling solution

A polypropylene mold was designed and fabricated via computer numerical control machining. Pristine PU standard samples (86 × 86 × 6 mm^3) were placed in a mold. Then, the mold containing the PU samples and filling solution were placed into a reaction flask (beaker flat bottom type) order-made, as shown in Fig. 1. The chamber was placed in a silicon oil bath to minimize the temperature gradient. For the accelerating aging test, four reaction flasks were heated to 50, 60, 70, and 80 °C. The specimen was obtained every 32, 16, 8, and 4 days, respectively. The obtained PU elastomers were wiped with polyester fabric and

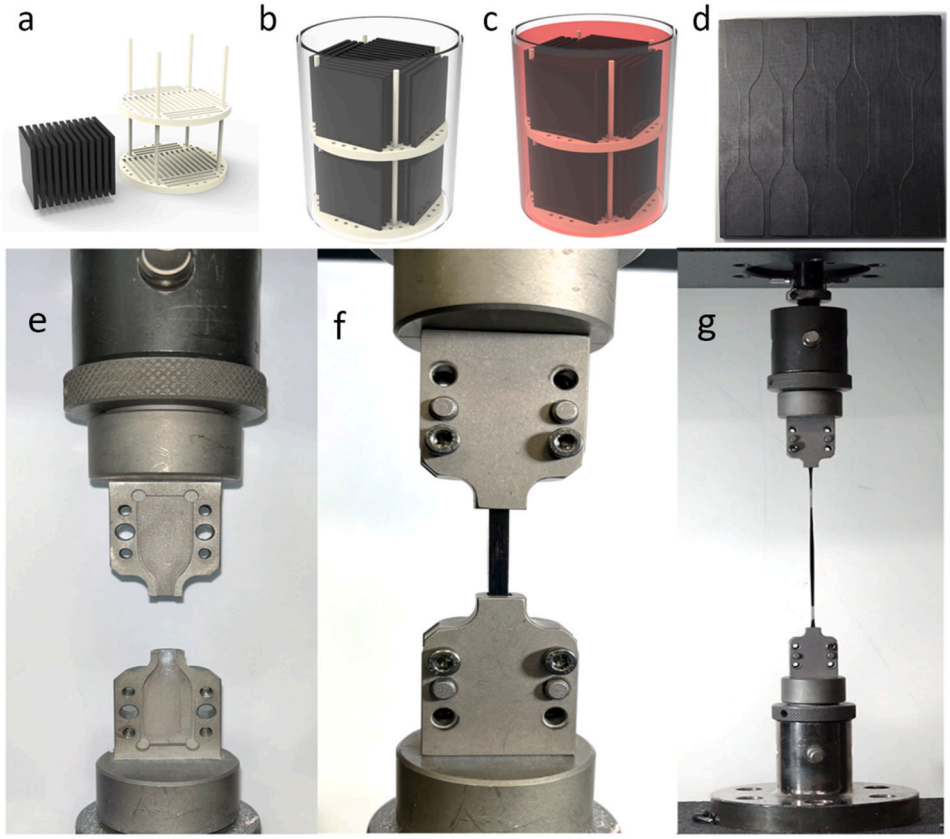

Fig. 1. Schematic of heat-aging test and Mechanical test of PU elastomer: (a) mold and PU elastomers, (b) PU elastomers in the heat-aging chamber, (c) PU elastomers in filling solution, (d) PU elastomer after dog-bone fabrication, (e) UTM grip, (f) PU elastomer loading into the grip, (g) PU elastomer during the tension test.

ethanol to clean the specimen surface. PU elastomers were stored in plastic bags. The filling solution consisted of ethylene glycol and water. Because freezing temperature is directly related to the reliability of the filling solution, the volume ratio of ethylene glycol:water is 2:1, because the freezing temperature of the solution reaches under −50 °C at that ratio [27].

2.3. Condition of experiment

The elongation at the break and the tensile strength were used as factors to predict the lifetime of the PU elastomers. The threshold point of the fracture was determined according to ASTM D2000. Dog-bone specimens were prepared after heat aging. The thickness of the dog-bone specimen was 6 mm and was processed following ISO 37-2017, with type 2 test specimens, but only grip parts were made larger than normal to prevent the slip of the specimen during the mechanical test.

2.4. FT-IR characterization

The chemical degradation of the pristine and heat-aged PU elastomer was studied using Fourier transform infrared (FT-IR) spectroscopy. The agglomerates of the decomposed PU elastomer were also inspected. FT-IR spectra were obtained using a Nicolet iS10 spectrometer (Thermo Fisher Scientific Inc., USA). The elastomers were dried in a vacuum oven before the inspection. The spectra were recorded in the range of 600–4000 cm^{-1} with 4 cm^{-1} resolution over 32 scans.

2.5. Thermogravimetric analysis (TGA)

Discovery TGA 55 (TA Instruments, DE) was used to analyze the onset decomposition temperature of the heat-aged PU elastomer. The TGA curve was obtained using a sample mass of about 20 mg, from 30 to 600 °C at a heating rate of 5 °C/min, under air condition.

2.6. Modulated differential scanning calorimetry (MDSC)

Discovery DSC 25 (TA Instruments, DE) was used to study about the effect of heat aging on mechanical properties. Cell constant and temperature were previously calibrated using indium. The data was obtained with oscillation amplitude of ±0.5 °C within a period of 120 s. Heating rate were 2 °C/min. The weight of specimen was in a range of 4.5–5.5 mg.

2.7. Mechanical properties

The effect of heat aging on the mechanical properties of the PU elastomer was evaluated using an Instron 5882 universal material testing machine (UTM) (Instron, UK). Stress–strain curves were collected at a strain speed of 500 mm/min. As shown in Fig. 1(e), compatible with UTM equipment, a specially designed grip was manufactured to prevent elastomer samples from falling out during tensile testing. The hardness of the PU elastomers was tested using a TIME® 5430 hardness tester (Beijing Time High Technology Ltd., China) with an operation stand. Hardness was estimated at eight points for each PU elastomer and averaged.

3. Result

3.1. Mechanical properties

PU elastomers were heat-aged at 80, 70, 60, and 50 °C. Heat aging was conducted in the filling solution. The solution was prepared with an ethylene glycol:water volume ratio of 2:1. Fig. 2(a) shows the increased weight ratio of the PU elastomer after exposure to the solution. The weight ratio was calculated by dividing the weight of the heat-aged PU elastomer by the average weight of the pristine PU elastomer.

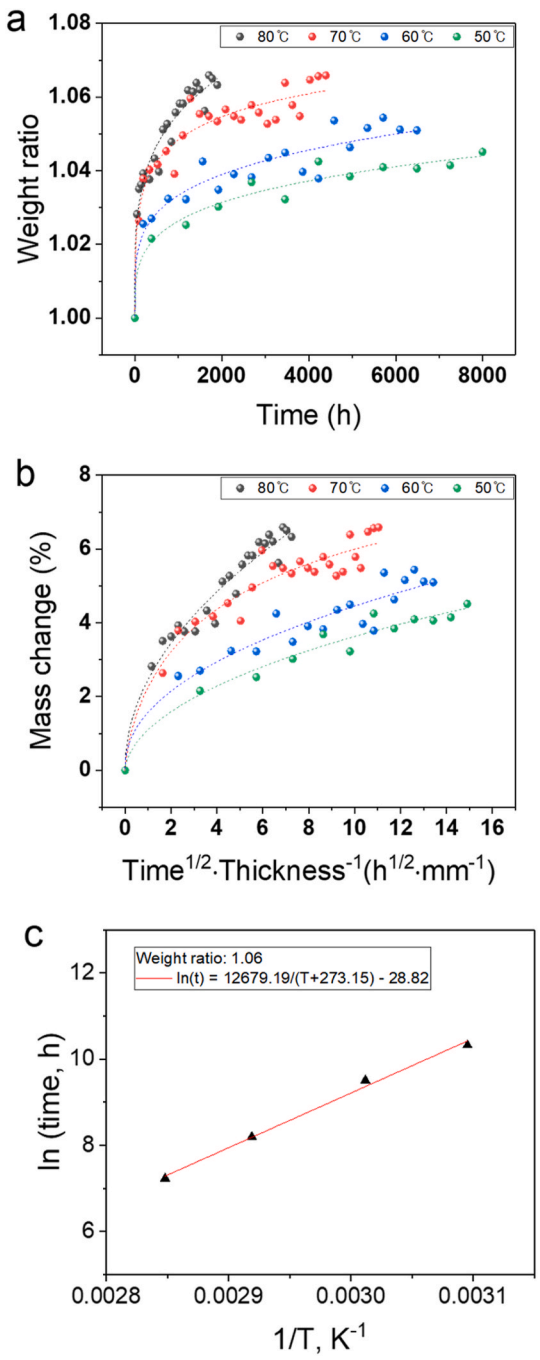

Fig. 2. Weight change in heat-aged PU elastomer in several temperatures: (a) as a function of heat-aging time, (b) as a function of root of time and inverse of thickness. (c) Arrhenius plotting of temperature and estimated time to reach saturation point.

The PU elastomer absorbed the filling solution over time and gained weight. The absorption of the solution at higher temperatures was greater than that at lower temperatures. At all temperatures, the elastomer largely absorbs the solution first, after which it exhibits a relatively slow absorption. The amount of filling solution saturated in the elastomer was larger at a higher heat-aging temperature. The large initial absorption may be ascribable to the diffusion of the solution into the PU elastomer. The slow absorption may originate from the micro-voids formed by the dissociation of urethane bonds in the PU elastomer.

Fig. 2(b) shows the Fickian behavior of the solution diffusion. The absorption of the uptake in the initial phase is proportional to the square

root of time and inversely proportional to the sample thickness. Subsequently, a plateau region is observed. The mass transfer equation from Fick's law can be simplified as follows [28,29].

$$\frac{\partial C}{\partial t} = D\left(\frac{\partial^2 C}{\partial x^2} + \frac{\partial^2 C}{\partial y^2} + \frac{\partial^2 C}{\partial z^2}\right) \quad (1)$$

where C is the molar concentration (mol/m^3), t is time (s), and D is the diffusion coefficient (m^2/s). As the PU elastomer has a planar shape, the majority of diffusion occurs in one direction. Thus, a possible model of solution absorption in PU elastomer is as follows:

$$\frac{\partial C}{\partial t} = D\frac{\partial^2 C}{\partial x^2} \quad (2)$$

The time required to reach the plateau region is expected to satisfy the Arrhenius equation. As shown in Fig. 2(a), the 80 and 70 °C heat-aged PU elastomer were saturated near the 1.06 ratio. Therefore, the time to reach the saturation point of 60 and 50 °C heat-aged PU elastomer was estimated using a trend line. The estimated times to reach a saturation point at 60 and 50 °C were 13,471 h and 30,468 h, respectively. The temperature dependence of the PU elastomer saturation is plotted in Fig. 2(c) and appears to follow Arrhenius plots. Le Gac et al. [30] emphasized that after heat-aging the PU elastomers in water, all specimens exhibited a constant value of maximum water uptake at all heat-aging temperatures. In addition, the kinetics of water uptake and temperature can be fitted using Arrhenius plots. Because the types of PU elastomer and filling solution are different, the saturation kinetics may be distinct. However, in both cases, the Arrhenius plot exhibited a linear trend, proving the temperature dependence of the diffusion kinetics.

The PU elastomer specimens subjected to heat-aging in the filling solution at 80, 70, 60, and 50 °C were weighed, processed into five dog-bone specimens, and then, the mechanical properties were measured. Fig. 3 shows the tensile strength and elongation at the break of the specimens. The tensile strength value (Fig. 3(a)) shows a rapid decrease in the initial section and then a tendency to stabilize. In the quick drop in the initial range, the rate of decline differed depending on the heat-aging temperature. At the 80 °C heat-aging conditions, the highest decrease in tensile strength is observed. At the end of the steep drop, the tensile strength values remain almost the same at 80, 70, and 60 °C heat-aging. This is attributable to the dissociation of the covalent and hydrogen bonds in the hard segment of the PU elastomer.

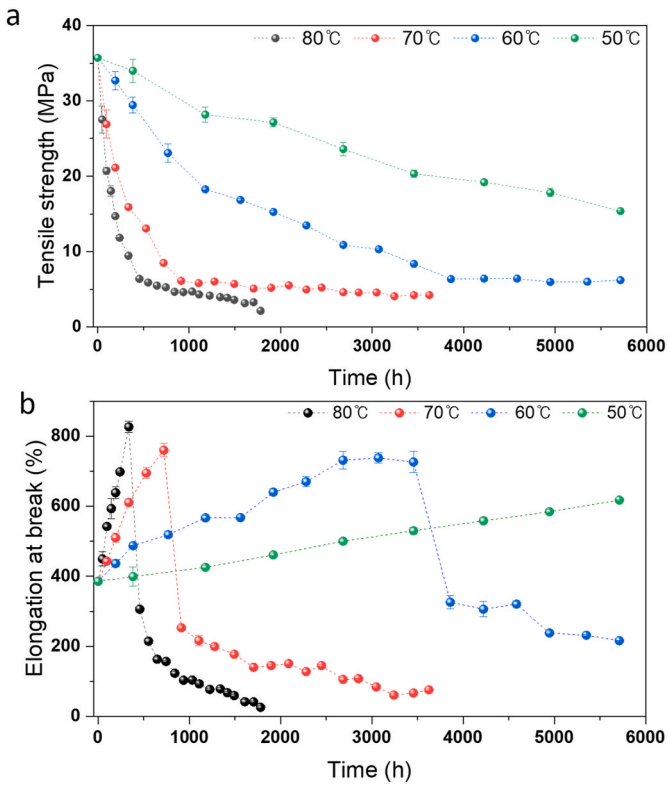

Fig. 3. Mechanical test of PU elastomer: (a) Tensile strength of PU elastomer as a function of heat-aging. (b) Elongation at the break of PU elastomer as a function of heat-aging time.

Similar results were obtained in the elongation and tensile strength tests. As shown in Fig. 3(b), the most rapid change occurs at 80 °C, and similar final values are acquired in all cases, except the 50 °C test. However, notably, unlike in the case of general elastomer, the elongation at the break initially showed an upward trend before a sharp decrease. For example, during heat-aging at 80 °C, the value of elongation at the break reaches a maximum at 336 h and decreases sharply when the heat-aging time passes from 336 to 456 h. Moreover, the tensile strength also reached the almost minimum value. This behavior may be due to changes in the hydrogen bonds between the hard segments and the cleavage of covalent bonds in the PU elastomer.

Fig. 4 shows how the hydrogen bonds between the hard segments are interrupted by a heat-aging time. In the case of pristine elastomer, the hard segment is well-packed by hydrogen bonding among the urethane bonds. It initially has sufficient hydrogen bonds between the hard segments. Thus, the elastomer has moderately low elongation. Additionally, because no cleavage of covalent bonds occurs because heat-aging is not performed, the tensile strength is the highest. However, during heat-aging up to 336 h, hydrogen bonds between hard segments are disrupted by water and ethylene glycol molecules. Thus, the number of hydrogen bonds between hard segments decreased. Moreover, water and ethylene glycol molecules enter between the hard segments and widen the distance and weaken the hydrogen bonds between them. The cleavage of covalent bonds in the hard segment is also another reason for changes in mechanical properties. With a small amount of cleavage, it provides additional chain flexibility by giving extra space for the polymer chain to move as well as additional elongation at the break [31,32].

However, when the covalent bond in the hard segments is further reduced, the tensile strength begins to decrease. After heat aging for 456 h, the urethane decomposition reaction broke more covalent bonds, so the network structure inside the PU elastomer could not be maintained. Therefore, the elongation at the break decreased sharply and the tensile strength reached a minimum value.

3.2. FT-IR, TGA and MDSC characterization

FT-IR measurements were performed to ensure that the above interpretation was accurate. Because the urethane bond with hydrogen bonding had a lower wavenumber than the urethane bond without hydrogen bonding, the interpretation could be verified through IR inspection.

The peak at 1732 cm^{-1} of the urethane bond shifted to 1712 cm^{-1} owing to hydrogen bonding [33]. As shown in Fig. 4(b), pristine elastomer without heat aging shows a relatively high-intensity peak at 1712 cm^{-1}. For the sample heat-aged at 80 °C for 336 h, before the elongation at the break sharply decreases, the peak intensity at 1712 cm^{-1} appears relatively small because the urethane bond inside the hard segment is less disturbed by the hydrogen bond. In the case of the specimen heat-aged for 456 h, almost no peak is observed at 1712 cm^{-1}. Similar or smaller peaks at 1712 cm^{-1} appear in samples with longer heat-aging times (744, 1224, and 1608 h).

Therefore, at the initial stage of heat-aging, hydrogen bonding between hard segments, which can also act as a cross-linking point, is disturbed; thus, elongation at the break increases and tensile strength decreases. However, after the phase, both the elongation at the break and tensile strength appeared to decrease owing to the cleavage of numerous covalent bonds.

However, in Fig. 4(c), the FT-IR spectrum of a sample after 1608 h of

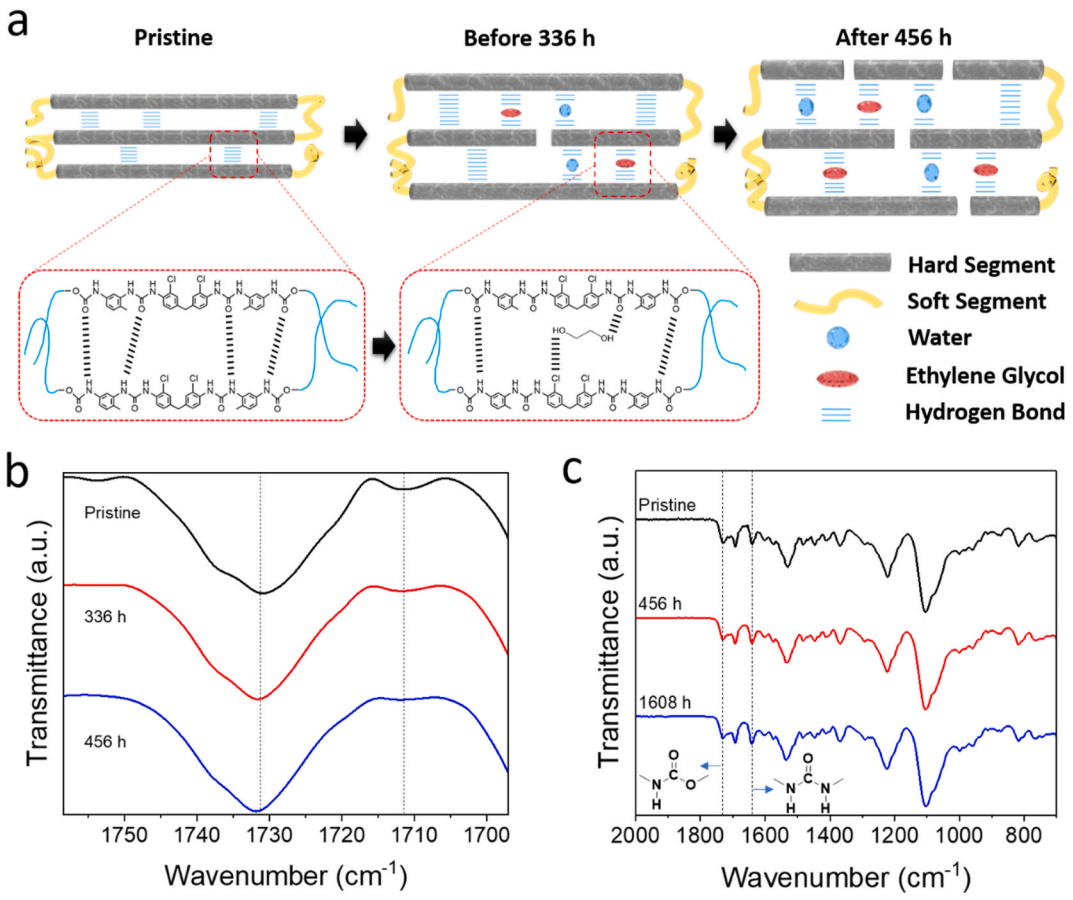

Fig. 4. (a) Diagram of hard segment and hydrogen bond in PU elastomer in different heat-aged hours. (b) FT-IR spectra of PU elastomer after 80 °C heat aging. Spectra show different intensities around 1712 cm^{-1}, which indicates that hydrogen bonds hindered the urethane bond between hard segments. (c) FTIR spectra of pristine PU elastomer and after 80 °C heat-aging (456, 1608 h).

heat-aging in the 80 °C filling solution shows that the intensity of the urethane C═O peak at 1732 cm^{-1} is almost the same as that of pristine. Moreover, the intensity of the urea C═O peak at 1640 cm^{-1} by the curing agent also does not show a significant difference between the aged and clean samples, which could explain the decrease in mechanical properties. To elucidate the results, the mechanism of the degradation reaction was investigated.

Under atmospheric pressure, hydrolysis requires significantly more energy, that is, in significantly harsher conditions, than glycolysis [34–37]. Therefore, PU elastomer undergoes more glycolysis than hydrolysis in the presence of both water and ethylene glycol. Moreover, the urea bond is easier to dissociate than the urethane bond by hydrolysis [38,39]. Therefore, it can be concluded that the urea bond is more degraded than the urethane bond via glycolysis because both hydrolysis and glycolysis have similar degradation mechanisms.

Fig. 5(a) shows the chemical degradation mechanism of the urethane and urea bonds via glycolysis. It is challenging to distinguish them using FT-IR spectroscopy because the urethane bonds remain intact after glycolysis. However, the urethane chain dissociated via glycolysis becomes shorter and has a structure that easily releases into the filling solution. When the urea bond is dissociated, it can be distinguished using FT-IR spectroscopy because the product of glycolysis is a primary amine.

As shown in Fig. 5(b), after 1608 h of heat-aging with the 80 °C filling solution, the filling solution was collected and centrifuged to obtain agglomerates of degraded PU elastomer. From the FT-IR measurements of the agglomerates, it can be inferred that there are $–NH_2$ peaks at 3442 and 3360 cm^{-1}. Because the peak of the urea bond at 1640 cm^{-1} disappears in the spectrum of the agglomerate, it is expected that $–NH_2$ is generated as the urea bond disappeared. In addition, the urethane peak of the agglomerate at 1732 cm^{-1} proves that the degradation of urea in the PU elastomer results in another urethane bond. This result indicates that the degradation of the PU elastomer is mainly attributed to the glycolysis of the urea bond, as shown in Fig. 5(a).

Thermogravimetric analyses were performed to study the effect of heat aging on thermal properties. Fig. 6 shows the changes in the onset decomposition temperature of PU elastomer, which was heat-aged at 80 °C, as a function of heat-aging time. The onset decomposition temperature is decreased as the heat-aging time increases at 80 °C. In a decreasing trend, there is an additional sharp drop between 336 and 456 h. Because this phase is a section where the rapid reduction in covalent bonds starts, this result is in accord with the FT-IR results.

The MDSC was used to study the effect of heat aging on mechanical properties in Fig. 7. Thermograms were analyzed to verify the effect of heat-aging on intermolecular interaction between hard segments. Non-reversing heat flow is related to kinetic events (degradation, crystallization, crystal perfection, recrystallization), and reversing heat flow is related to heat capacity events (glass transition and melting).

$$\frac{dH}{dt} = C_p(T)\frac{dT}{dt} + f(T,t) \quad (3)$$

Where dH/dt is total heat flow rate and C_p is the measured specific heat capacity related to the reversing heat flow and f (T, t) is related to the kinetic (non-reversing) component of the total heat flow. Non-reversing heat flow of aged PU elastomer shows an endothermic peak at around 193 °C. Dickie et al. [40] emphasized that this peak is not a melting peak but a breakup of the crystalline phase by depolymerization. Therefore, the 2nd cycle of DSC shows no endothermic peak at around 193 °C

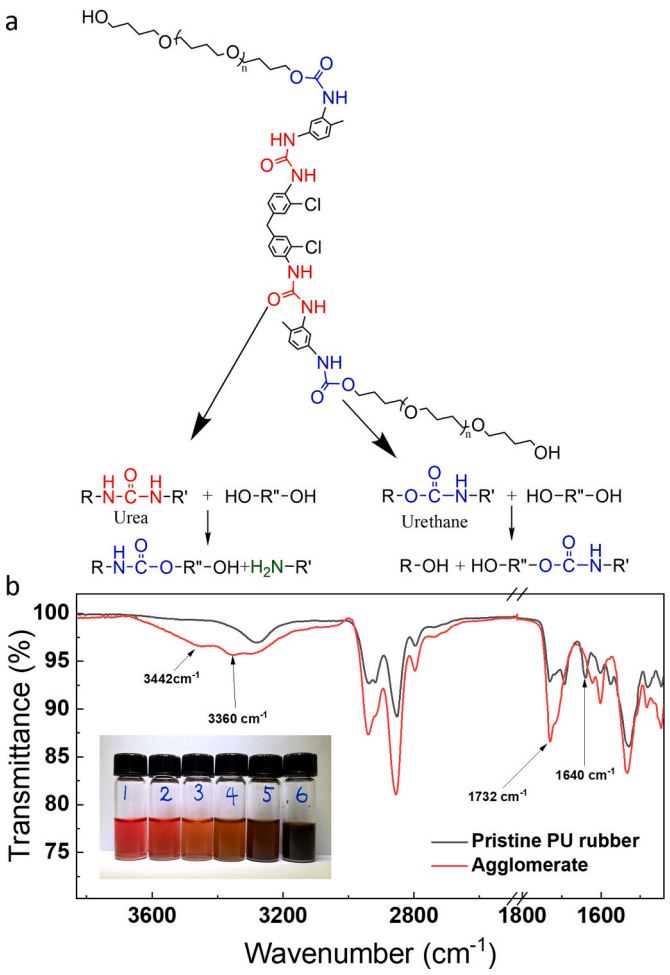

Fig. 5. (a) Mechanisms of heat-aging at PU elastomer in filling solution, (b) FT-IR spectra of pristine PU elastomer and agglomerate. Solution 1 is a pure filling solution, and solutions 2–5 are from heat-aged for 1608 h at 50, 60, 70, and 80 °C, respectively. Solution 6 is obtained via centrifugation of solution 5. Agglomerate was collected by drying solution 6.

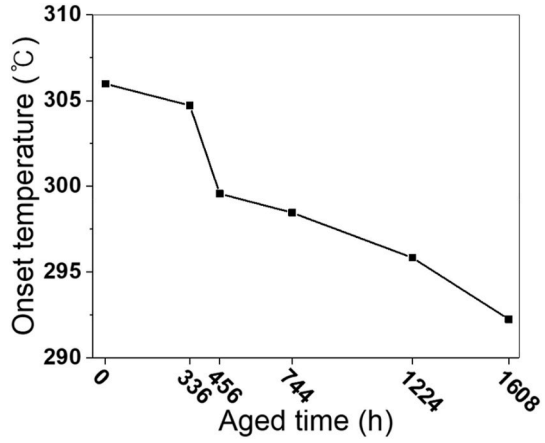

Fig. 6. Effect of 80 °C heat-aging time on the onset decomposition temperatures of PU elastomer (heating rate of 5 °C/min).

(Fig. S3). The area of the peak made by depolymerization is calculated in Fig. 7(f). The enthalpy of depolymerization is decreased by the time of heat aging. It can be inferred that as the heat-aging time increases, the amount of the crystalline phase which can be broken in PU elastomer is decreased. This may attribute to dissociation of the covalent bond of a hard segment which is a highly crystalline area. Furthermore, the decrease of slope in Fig. 7(f) is largest between 336 h and 456 h. This result is in accord with the mechanical properties data.

3.3. Calculated lifetime prediction of PU elastomer

ASTM D 2000 is the standard for classifying the lifespan of elastomer products. For the tensile strength and elongation, the lifespan is the time required to reach 70% and 50% of the initial values, respectively. As the tensile strength of pristine PU elastomer is 35.71 ± 3.61 MPa and the elongation at the break is 385.7% ± 16.4%, the threshold of fractures is 25.00 MPa and 192.85%, respectively.

The Arrhenius equation is often used to evaluate the tensile strength and elongation at the break of elastomers over a long period [41–44]. This equation is often used to determine the effects of aging. Therefore, the lifespan was predicted in this study using the Arrhenius equation. The aging rate of the PU elastomer can be expressed using the Arrhenius equation:

$$K(T) = A \bullet e^{\frac{-E_a}{RT}}, \text{ or } \ln(K(T)) = B - \left(\frac{E_a}{RT}\right) \quad (4)$$

where A is a pre-exponential factor, E_a is the activation energy, R is the gas constant, T is the absolute temperature, and K(T) is the time required to reach a specific physical property. Here, it was the time required to reach a tensile strength of 25.00 MPa and an elongation at the break of 192.85%. If a graph is drawn using the temperature and time required for tensile strength and elongation to reach a specific point, a straight line is plotted. As shown in Fig. 8, and the lifespan of elastomer at room temperature can be predicted using this straight line.

A straight line is observed by plotting the logarithm of the lifetime at a specific temperature against the reciprocal temperature. The lifespan at room temperature can be predicted via the straight-line trend. Table 1 lists the predicted lifespans of the heat-aged PU elastomer at 20 and 25 °C. In addition, the activation energy of degradation can be calculated using the slopes of the graphs. Activation energies calculated from tensile strength and elongation at the break graph are 118.0 and 124.1 kJ $mol^{-1}K^{-1}$, respectively.

The calculated lifetimes showed significantly different values, depending on the threshold. For lifespan estimation by elongation at the break, the lifespan is > 100 years at room temperature. However, the elongation at the break increased in the initial stage of heat-aging. Therefore, it is challenging to apply the elongation at the break standard to the PU elastomer. However, the lifespan determined using the tensile strength was >10 years at room temperature. When solution absorption and chemical degradation were considered, lifetime estimation based on tensile strength was more appropriate for practical use to prevent severe damage.

4. Conclusion

PU elastomer was fabricated and subjected to the accelerated heat-aging at different temperatures from 50 to 80 °C to determine the lifespan of elastomer in a water-glycol mixture at room temperature. The mechanical properties were obtained using a specially designed grip tool with UTM. In addition, chemical and thermal analyses were conducted. The tensile strength was decreased with the different rates depending on the temperature. In the case of elongation, it showed a tendency to increase initially, and then showed a rapid decrease. To explain these changes in tensile strength and elongation, FT-IR analysis was conducted for PU elastomer and agglomerates in the solution. Through this, it was possible to suggest the hydrogen bond change and decomposition mechanism in the hard segment region according to the aging time. The change in tensile strength was also correlated with the thermal analysis results. In the TGA results, the decomposition onset temperature

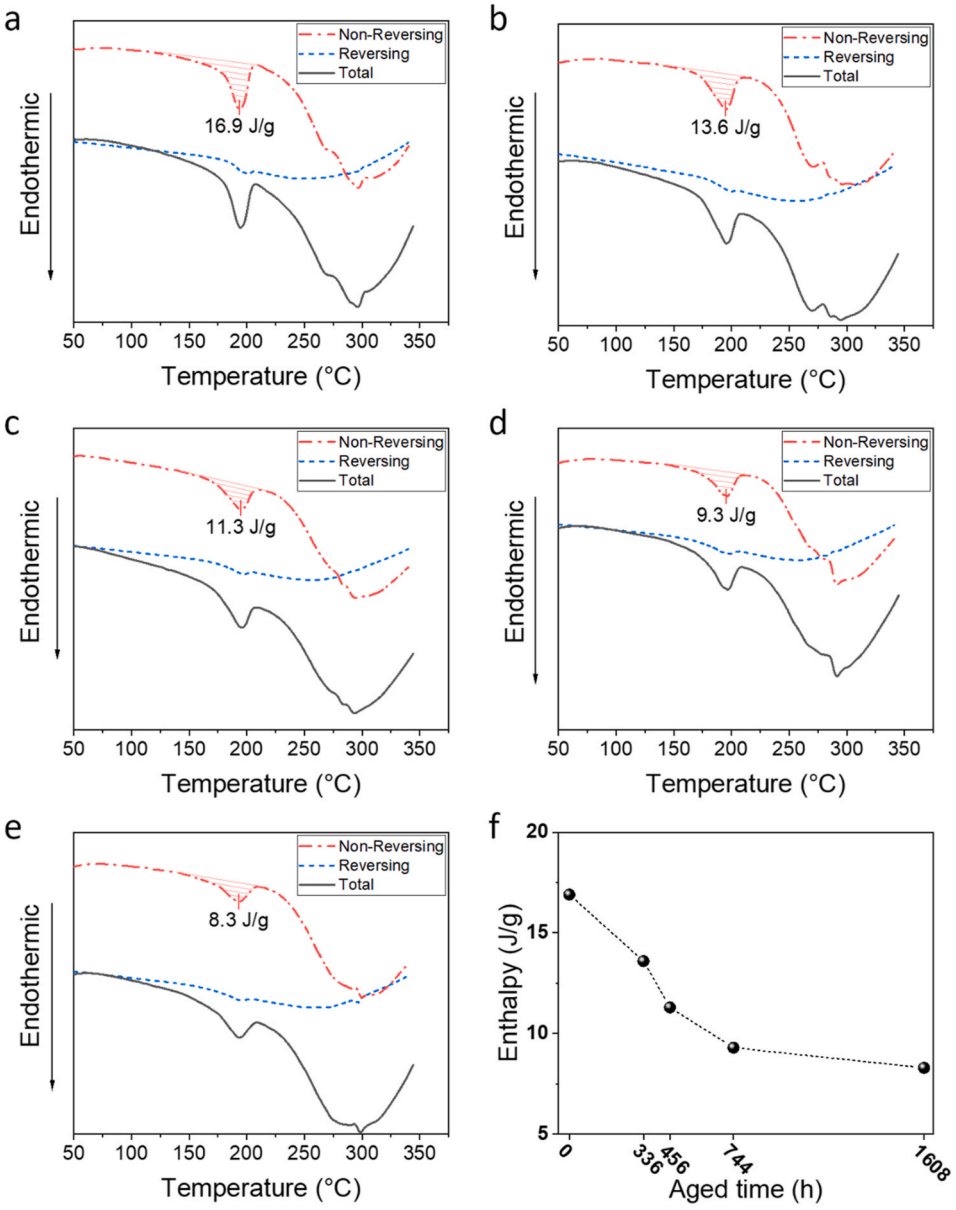

Fig. 7. MDSC data of heat aged elastomer: (a) pristine, (b) 336 h, (c) 456 h, (d) 744 h, (e) 1608 h, and (f) calculated enthalpy of non-reversing heat flow at around 193 °C.

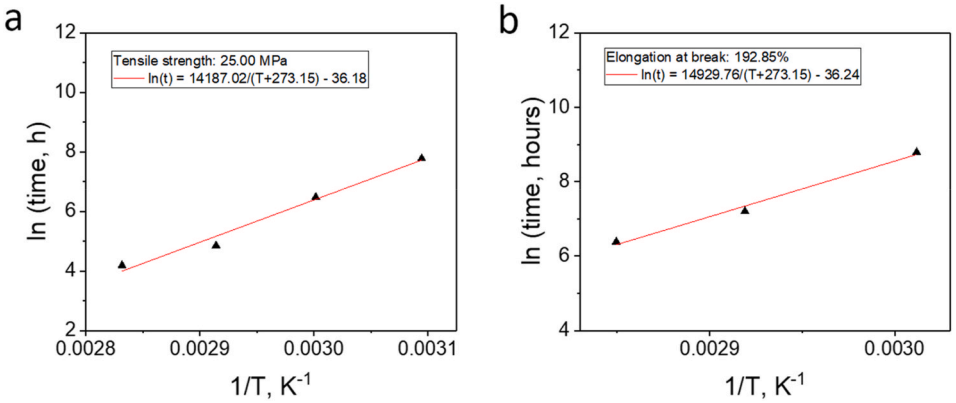

Fig. 8. Arrhenius plotting of temperature and time to reach fracture threshold: (a) tensile strength value of 25.00 MPa, (b) elongation at break value of 192.85%. At 50 °C heat-aging, elongation of PU elastomer did not reach 192.85% because of slow reaction.

Table 1
Calculated lifetime prediction of PU elastomer at room temperature.

Temperature (°C)	Lifetime prediction by tensile strength 25.00 MPa (year)	Lifetime prediction by Elongation 192.85% (year)
20	28.7	273.9
25	12.2	116.6

significantly decreased from 336 to 465 h, and in the MDSC data, depolymerization of the crystalline region occurred rapidly at the same time section. Finally, the lifetime of PU elastomer at room temperature was calculated using the Arrhenius equation based on the time required to reach the fracture threshold during thermal aging. Failure thresholds were determined according to ASTM D2000 specifications. The estimated lifetime based on the tensile strength standard is 12.2 years at room temperature. These results can suggest a certificate and inspection period for PU elastomer applications. In addition, we can make a new PU more durable and reliable for specific fields by understanding their molecular structure and functional units related to depolymerization.

Declaration of competing interest

The authors declare that they have no known competing financial interests or personal relationships that could have appeared to influence the work reported in this paper.

Data availability

No data was used for the research described in the article.

Acknowledgment

This research was supported by a National Research Foundation of Korea (NRF) grant (no. 2020R1C1C1012581) and the Principal Research Program PNK9330 in the Korea Institute of Materials Science (KIMS).

Appendix A. Supplementary data

Supplementary data to this article can be found online at https://doi.org/10.1016/j.polymertesting.2023.108086.

References

[1] R. Dinato, R. Cruz, R. Azevedo, J. Hasegawa, R. Silva, A. Ribeiro, A. Lima-Silva, R. Bertuzzi, Footwear designed to enhance energy return improves running economy compared to a minimalist footwear: does it matter for running performance? Braz. J. Med. Biol. Res. 54 (2021), e10693.
[2] N. Jirapongpathai, S. Sukthomya, P. Winyouvijit, K. Permpool, B. Inprang, F. R. Utama, H.T. Nugroho, Pilot study: the effects of air-filled thermoplastic polyurethane (TPU) in foot orthosis, Sci. Technol. Aliment. (2022) 209–216.
[3] J.O. Akindoyo, M. Beg, S. Ghazali, M. Islam, N. Jeyaratnam, A. Yuvaraj, Polyurethane types, synthesis and applications–a review, RSC Adv. 6 (2016) 114453–114482.
[4] E. Delebecq, J.-P. Pascault, B. Boutevin, F. Ganachaud, On the versatility of urethane/urea bonds: reversibility, blocked isocyanate, and non-isocyanate polyurethane, Chem. Rev. 113 (2013) 80–118.
[5] M.P.C. Blasco, M.Á.P. Limiñana, C.R. Silvestre, E.O. Calpena, F.A. Aís, Sustainable reactive polyurethane hot melt adhesives based on vegetable polyols for footwear industry, Polymers 14 (2022) 284.
[6] G. Stack, J. Miller, E. Chang, Development of seawater-resistant polyurethane elastomers for use as sonar encapsulants, J. Appl. Polym. Sci. 42 (1991) 911–923.
[7] A.J. Williams, F.T. Thwaites, Urethane Potting of Acoustic Transducers for Acoustic Travel-Time Current Meters, 2013 Ocean Electronics (SYMPOL), IEEE, 2013, pp. 1–11.
[8] M.E. Schinault, S.M. Penna, H.A. Garcia, P. Ratilal, Investigation and Design of a Towable Hydrophone Array for General Ocean Sensing, OCEANS 2019-Marseille, IEEE, 2019, pp. 1–5.
[9] Z. Chen, G. Yao, Analysis of Radar and Infrared Stealth Compatibility Design for Surface Ships, IOP Conference Series: Earth and Environmental Science, IOP Publishing, 2019, 052132.
[10] R.G. Hunt, W.E. Franklin, C.C. Hildebrandt, G.H. Buchanan, K.K. Hoffsommer, Life Cycle Assessment of Ethylene Glycol and Propylene Glycol Antifreeze, SAE Technical Paper, 1996.
[11] W. Zheng, L. Xu, Y. Li, Y. Huang, B. Li, Z. Jiang, G. Gao, Anti-freezing, moisturizing, resilient and conductive organohydrogel for sensitive pressure sensors, J. Colloid Interface Sci. 594 (2021) 584–592.
[12] P. Zahedifar, L. Pazdur, C.M. Vande Velde, P. Billen, Multistage chemical recycling of polyurethanes and dicarbamates: a glycolysis–hydrolysis demonstration, Sustainability 13 (2021) 3583.
[13] P. Kanchanapiya, N. Intaranon, T. Tantisattayakul, Assessment of the economic recycling potential of a glycolysis treatment of rigid polyurethane foam waste: a case study from Thailand, J. Environ. Manag. 280 (2021), 111638.
[14] S. Taourit, P.-Y. Le Gac, B. Fayolle, Relationship between network structure and ultimate properties in polyurethane during a chain scission process, Polym. Degrad. Stabil. 201 (2022), 109971.
[15] H. Zhang, G. Han, W. Cheng, S. Liu, X. Wang, Incorporation of CO2-polyols into ester-based waterborne polyurethane: an effective strategy to improve overall performance, J. Appl. Polym. Sci. 139 (2022), e52661.
[16] O. Trhlíková, V. Vlčková, S. Abbrent, K. Valešová, L. Kanizsová, K. Skleničková, A. Paruzel, S. Bujok, Z. Walterová, P. Innemanová, Microbial and abiotic degradation of fully aliphatic polyurethane foam suitable for biotechnologies, Polym. Degrad. Stabil. 194 (2021), 109764.
[17] L. Yuan, W. Zhou, Y. Shen, Z. Li, Chemically recyclable polyurethanes based on bio-renewable γ-butyrolactone: from thermoplastics to elastomers, Polym. Degrad. Stabil. 204 (2022), 110116.
[18] S. Nilawar, K. Chatterjee, Olive oil-derived degradable polyurethanes for bone tissue regeneration, Ind. Crop. Prod. 185 (2022), 115136.
[19] X. Xu, Y. Yuan, S. Jin, Z. Han, C. Liang, H. Zhu, Study on polyurethane elastomer modification for improving low-temperature resistance of high-capacity polyurethane elastomeric bearing for bridges, Construct. Build. Mater. 347 (2022), 128625.
[20] J. Zhang, X. Guo, X. Zhang, H. Wang, J. Zhu, Z. Shi, S. Zhu, Z. Cui, Hydrolysis-resistant and stress-buffering bifunctional polyurethane adhesive for durable dental composite restoration, R. Soc. Open Sci. 7 (2020), 200457.
[21] E. Kong, B. Yoon, J.-D. Nam, J. Suhr, Accelerated aging and lifetime prediction of graphene-reinforced natural rubber composites, Macromol. Res. 26 (2018) 998–1003.
[22] P. Davies, Towards more representative accelerated aging of marine composites, in: Advances in Thick Section Composite and Sandwich Structures, Springer, 2020, pp. 507–527.
[23] V. Nikolic, R. Polansky, Assessing the Reliability of Electrical Insulating Materials Using Accelerated Aging Tests, 2020 International Conference on Diagnostics in Electrical Engineering (Diagnostika), IEEE, 2020, pp. 1–4.
[24] G. Hota, W. Barker, A. Manalo, Degradation mechanism of glass fiber/vinylester-based composite materials under accelerated and natural aging, Construct. Build. Mater. 256 (2020), 119462.
[25] M. Frigione, A. Rodríguez-Prieto, Can accelerated aging procedures predict the long term behavior of polymers exposed to different environments? Polymers 13 (2021) 2688.
[26] P.L. Bégin, E. Kaminska, Thermal Accelerated Ageing Test Method Development, 2002.
[27] Å. Melinder, Thermophysical Properties of Aqueous Solutions Used as Secondary Working Fluids, KTH, 2007.
[28] E. Richaud, B. Flaconnèche, J. Verdu, Biodiesel permeability in polyethylene, Polym. Test. 31 (2012) 1070–1076.
[29] N. Fredj, S. Cohendoz, S. Mallarino, X. Feaugas, S. Touzain, Evidencing antagonist effects of water uptake and leaching processes in marine organic coatings by gravimetry and EIS, Prog. Org. Coating 67 (2010) 287–295.
[30] P.-Y. Le Gac, D. Choqueuse, D. Melot, Description and modeling of polyurethane hydrolysis used as thermal insulation in oil offshore conditions, Polym. Test. 32 (2013) 1588–1593.
[31] Z. Cheng, Q. Li, Z. Yan, G. Liao, B. Zhang, Y. Yu, C. Yi, Z. Xu, Design and synthesis of novel aminosiloxane crosslinked linseed oil-based waterborne polyurethane composites and its physicochemical properties, Prog. Org. Coating 127 (2019) 194–201.
[32] G. Lligadas, J.C. Ronda, M. Galià, V. Cádiz, Poly (ether urethane) networks from renewable resources as candidate biomaterials: synthesis and characterization, Biomacromolecules 8 (2007) 686–692.
[33] E. Yilgör, E. Burgaz, E. Yurtsever, I. Yilgör, Comparison of hydrogen bonding in polydimethylsiloxane and polyether based urethane and urea copolymers, Polymer 41 (2000) 849–857.
[34] A. Nemade, S. Mishra, V. Zope, Kinetics and thermodynamics of neutral hydrolytic depolymerization of polyurethane foam waste using different catalysts at higher temperature and autogenious pressures, Polym.-Plast. Technol. 49 (2009) 83–89.
[35] L.R. Mahoney, S.A. Weiner, F.C. Ferris, Hydrolysis of polyurethane foam waste, Environ. Sci. Technol. 8 (1974) 135–139.
[36] A. Aguado, L. Martínez, A. Moral, J. Fermoso, R. Irusta, Chemical recycling of polyurethane foam waste via glycolysis, Chem. Eng. Transact 24 (2011) 1069–1074.
[37] M. Murai, M. Sanou, T. Fujimoto, F. Baba, Glycolysis of rigid polyurethane foam under various reaction conditions, J. Cell. Plast. 39 (2003) 15–27.
[38] J. Sahu, K. Mahalik, A. Patwardhan, B. Meikap, Equilibrium and kinetic studies on the hydrolysis of urea for ammonia generation in a semibatch reactor, Ind. Eng. Chem. Res. 47 (2008) 4689–4696.

[39] K.A. Chaffin, X. Chen, L. McNamara, F.S. Bates, M.A. Hillmyer, Polyether urethane hydrolytic stability after exposure to deoxygenated water, Macromolecules 47 (2014) 5220–5226.
[40] B. Dickie, Investigation of an engineering thermoplastic polyurethane by MDSC, Thermochim. Acta 304 (1997) 347–352.
[41] S.M. Imran, C. Li, L. Lang, Y. Guo, H.A. Mirza, F. Haq, S. Alexandrova, J. Jiang, H. Han, An investigation into Arrhenius type constitutive models to predict complex hot deformation behavior of TC4 alloy having bimodal microstructure, Mater. Today Commun. 31 (2022), 103622.
[42] J. Wise, K. Gillen, R. Clough, An ultrasensitive technique for testing the Arrhenius extrapolation assumption for thermally aged elastomers, Polym. Degrad. Stabil. 3 (1995) 403–418.
[43] M.H. Keshavarz, M. Karimi, E. Goodarzi, S.H. Hosseini, The use of the change of elongation for comparison of the shelf life of composite solid propellants in the air and nitrogen atmospheres, Z. Anorg. Allg. Chem. 647 (2021) 696–703.
[44] A.O. Mosleh, A.D. Kotov, A.A. Kishchik, O.V. Rofman, A.V. Mikhaylovskaya, Characterization of superplastic deformation behavior for a novel Al-Mg-Fe-Ni-Zr-Sc alloy: Arrhenius-based modeling and artificial neural network approach, Appl. Sci. 11 (2021) 2208–2227.